Title

Opponent Learning with Different Representations in the Cortico-Basal Ganglia Pathways Can Develop Obsession-Compulsion Cycle

Short title

Opponent dual cortico-basal ganglia circuits and obsession-compulsion

Author names and affiliations

Reo Sato[1+], Kanji Shimomura[1+], & Kenji Morita[1,2*]

[1] Physical and Health Education, Graduate School of Education, The University of Tokyo, Tokyo 113-0033, Japan

[2] International Research Center for Neurointelligence (WPI-IRCN), The University of Tokyo, Tokyo 113-0033, Japan

[+] These authors contributed equally to this work.

**Corresponding author*

Kenji Morita, Ph.D. (ORCID iD: orcid.org/0000-0003-2192-4248)

Physical and Health Education, Graduate School of Education, The University of Tokyo

7-3-1 Hongo, Bunkyo-ku, Tokyo 113-0033, Japan

morita@p.u-tokyo.ac.jp

Author contributions

KM conceived of the possibility that combined SR- and IR-based systems could develop OCD-like behavior, and elaborated the idea in discussion with RS and KS. RS, KS, and KM conducted/validated the simulations and analyses. KM drafted the manuscript, and revised it with inputs from RS and KS. According to the CRediT Taxonomy, Conceptualization: KM; Investigation: RS, KS, KM; Funding Acquisition: KM; Writing – Original Draft Preparation: KM; Writing – Review & Editing: RS, KS, KM.

Acknowledgements

KM was supported by Grant-in-Aid for Scientific Research (No. 20H05049) of the Ministry of Education, Culture, Sports, Science and Technology in Japan (MEXT) (http://www.mext.go.jp/en/) and the Japan Society for the Promotion of Science (JSPS) (https://www.jsps.go.jp/english/) and the Naito Foundation (https://www.naito-f.or.jp/en/).

Conflict of interest

None

Abstract

Obsessive-compulsive disorder (OCD) has been suggested to be associated with impairment of model-based behavioral control. Meanwhile, recent work suggested shorter memory trace for negative than positive prediction errors (PEs) in OCD. Relation between these two suggestions remains unclear. We addressed this issue through computational modeling. Based on the properties of cortico-basal ganglia pathways, we modeled human as agent having a combination of successor representation (SR)-based system that enables model-based-like control and individual representation (IR)-based system that only hosts model-free control, with the two systems potentially learning from positive and negative PEs in different rates. We simulated the agent's behavior in the environmental model used in the recent work that describes potential development of obsession-compulsion cycle. We found that the dual-system agent could develop enhanced obsession-compulsion cycle, similarly to the agent having shorter memory trace for negative PEs in the recent work, if the SR- and IR-based systems learned mainly from positive and negative PEs, respectively. We then simulated the behavior of such an opponent SR+IR agent in the two-stage decision task, in comparison with agent having only SR-based control. Fitting of the agents' behavior by the model weighing model-based and model-free controls developed in the original two-stage task study resulted in smaller weights of model-based control for the opponent SR+IR agent than for the SR-only agent. These results reconcile the previous suggestions about OCD, i.e., impaired model-based control and shorter memory trace for negative PEs, raising a novel possibility that opponent learning in model(SR)-based and model-free controllers underlies obsession-compulsion. Moreover, together with a recent suggestion that the opponent SR+IR combination actually performs well in certain dynamic environments and its cortico-striatal implementation appears consistent with several physiological/anatomical findings, this possibility explains why human is prone to OCD and even healthy people tended to show shorter memory trace for negative PEs.

Author summary

Obsessive-compulsive disorder (OCD) is one of the major psychiatric disorders diagnosed in 2.5%-3% of the population, and is characterized as an enhanced cycle of obsessive thought, e.g., whether the door was locked, and compulsive action, e.g., checking door lock. It remains elusive why such an apparently maladaptive behavior could be enhanced. A prevailing theory proposes that humans use two control systems, flexible yet costly goal-directed system and inflexible yet costless habitual system, and impairment of the goal-directed system leads to OCD. On the other hand, recent work proposed a new theory that shorter memory trace for credit-assignment of negative, than positive, prediction errors can induce OCD. Relation between these two theories remains unclear. We show that opponent learning of particular type of goal-directed(-like) system, suggested to be implemented in the brain, and habitual system from positive versus negative prediction errors could exhibit an (apparent) overall decrease in goal-directed control and also develop enhanced obsession-compulsion cycle similar to the one developed by memory-trace imbalance, thereby bridging the two theories. Such an opponent learning of the two systems was actually suggested to be advantageous in certain dynamic environments, and could thus be evolutionarily selected at the cost of possible development of OCD.

Introduction

Obsessive-compulsive disorder (OCD) has been suggested to be associated with impairment of model-based/goal-directed behavioral control, as compared to model-free/habitual control [1-4]. In the two-stage decision task with reward or no-reward outcomes [5], OCD patients showed impaired model-based choices [2, 3]. Also, deficits in model-based control in the two-stage task were strongly associated with a symptom dimension "compulsive behavior and intrusive thought" in the general population [5]. Meanwhile, recent work [6] suggested that memory trace imbalance underlies OCD. Specifically, modeling showed that obsession-compulsion cycle can be enhanced in agent having much shorter memory (eligibility) trace for negative than positive prediction errors (PEs), and fitting of behavioral choices suggested that OCD patients indeed had such an imbalance as compared to healthy controls (HCs), although even HCs tended to show shorter memory trace for negative than positive PEs. Mechanisms of such memory trace imbalance, as well as its relation to the suggestion of impaired model-based control, remain unclear.

Whereas the abovementioned modeling in the recent work [6] examined agent that only had model-free control, multiple studies have suggested that humans and other animals use both model-based and model-free controls [7, 8]. Model-free control has been suggested to be implemented in the way that dopamine represents reward PEs (RPEs) and dopamine-dependent plasticity of cortico-striatal synapses represents RPE-based update of state/action values [9, 10]. Neural implementation of model-based control has remained more elusive, but recent studies suggest that if states or actions are represented in a manner that contains information about action-state transitions, partially model-based-like control can be acquired through RPE-based update and thereby through dopamine-dependent plasticity, similarly to model-free control [11]. As such a representation, successor representation (SR), in which state/action is represented by cumulative occupancies of successor states/actions (Figure 1A) [12], has been suggested to be used in humans [13] and implemented in the brain [14-16].

Different cortical regions or neural populations may adopt different ways of representations, in particular, SR and more classical individual (punctate) representation (IR), and they may unevenly project to and/or activate the direct and indirect pathways of basal ganglia [17-19], which have been suggested to be crucial for learning from positive and negative feedbacks, respectively [20-25] (Figure 1B). Different circuits for positive and negative learning other than these pathways have also been suggested [26, 27]. Given these, it is conceivable that SR-based system and IR-based system differentially learn from positive and negative RPEs in the brain (Figure 1C). Recent work [28] explored this possibility, and found that combination of SR- and IR-based systems learning mainly from positives and negative RPEs, respectively (referred to as appetitive SR- and aversive IR-based systems), performed well in certain dynamic reward environments. This work further suggested that implementation of such a combination in the cortico-basal ganglia pathways seems in line with various

anatomical and physiological findings, including activations indicative of SR in limbic or visual cortices [15, 16] and preferential connections from limbic and visual cortices to the direct pathway of basal ganglia [18, 19].

Crucially, SR has a similarity to the eligibility trace (c.f., its "forward view" [29]) while model-free learning without eligibility trace is naturally described by using IR. Given this correspondence, we expected that the combination of appetitive SR- and aversive IR-based systems could potentially show similar behavior to the one shown by the agent having long / short eligibility traces for positive / negative RPEs in the abovementioned recent work [6], in particular, enhancement of obsession-compulsion cycle. Moreover, we also expected that fitting of behavior of the agent with combined appetitive SR- and aversive IR-based systems could potentially result in smaller weights of model-based control than the agent with SR-based system only in the two-stage decision task [7], which was used to estimate the degree of model-based/free control in many studies including those examining OCD or obsessive-compulsive symptoms [3, 5], whereas eligibility-trace imbalance *per se* would not bias the estimation of the degree of model-based control. Here we addressed these expectations.

Results

Environmental model and dual-system agent

We adopted the previously developed environmental model that describes possible enhancement of obsession-compulsion cycle [6] (Figure 2). There are two states named the relief state and the obsession state. At the relief state, agent can take one of two actions named the "abnormal reaction" and the "other" action. Here it is presumed that occasionally some anxiety e.g., about whether the door was locked arises spontaneously (intrusive thought), and agent can either get deeply into the anxiety ("abnormal reaction"), entering the obsession state, or just ignore or forget about it and do other things ("other" action), remaining in the relief state. Once agent enters the obsession state, agent again can take one of two actions. If agent takes the "compulsion" action by paying a small cost, e.g., confirms door lock, agent can transition back to the relief state with a high probability. Alternatively, agent can take "other" action without any cost, but it makes the agent transition back to the relief state only with a small probability. Every stay at the obsession state imposes punishment (negative reward).

Because of this punishment and also the cost, the optimal value of the obsession state should be negative and lower than the optimal value of the relief state. Thus, the optimal value of the "abnormal reaction", which induces transition to the obsession state, should be negative and lower than the optimal value of the "other" action at the relief state. Therefore, normative reinforcement learning (RL) agent should learn a policy that minimizes selection of the "abnormal reaction", thereby never developing enhanced obsession-compulsion cycle. However, agent that deviates from normative RL, such as the one having different lengths of eligibility traces for positive versus negative RPEs examined in the previous work [6], may behave differently.

We examined how the dual-system agent having coupled SR- and IR-based systems (Figure 1C), originally developed in [28], behaved in this environmental model. As mentioned in the Introduction (and also in [28]), this dual-system agent was motivated by the suggestions that humans/animals use both model-based (SR-based) and model-free (IR-based) controls, which may learn differently from positive and negative RPEs through uneven projections from different cortical populations hosting different representations (SR or IR) to the direct and indirect pathways of basal ganglia. In this dual-system agent, each system develops the system-specific value of each action, and the average of the two system-specific values, named the (integrated) action value, is used for soft-max action selection and calculation of RPEs. The RPEs are used for updating the system-specific values, with the learning rates for the SR- and IR-based systems in the cases of positive and negative RPEs, denoted as α_{SR+}, α_{SR-}, α_{IR+}, and α_{IR-}, allowed to take different values.

Behavior of the dual-system agent in the environmental model

First, we confirmed whether agent that effectively had only the IR-based system with the same learning rates from positive and negative RPEs, i.e., conventional model-free agent, behaved in the normative manner as described above, by setting the learning rates of the SR-based system from positive and negative RPEs (α_{SR+} and α_{SR-}) to 0 while α_{IR+} and α_{IR-} were set to 0.1. Figure 3A-top shows an example of the time evolution of the difference in the (integrated) action values of "abnormal reaction" and "other" at the relief state ($Q_{abnormal} - Q_{other@relief}$). Figure 3A-middle shows the moving average of the proportion that the agent was at the obsession state in the same example simulation, and Figure 3A-bottom shows the average of such a moving-average proportion across 100 simulations. As shown in these figures, it was confirmed that this agent minimized selection of the "abnormal reaction" at the relief state and never developed enhanced obsession-compulsion cycle. We next examined the case where agent effectively had only the SR-based system with unbiased learning from positive and negative PREs, by setting α_{IR+} and α_{IR-} to 0 while α_{SR+} and α_{SR-} were set to 0.1. As shown in Figure 3B, this agent also minimized selection of the "abnormal reaction". This is actually reasonable given that SR-based temporal-difference (TD) leaning can generally approximate optimal value functions.

Next, we examined the behavior of agent in which both IR-based system and SR-based system were effective and the learning rate was all equal for both systems and also for positive and negative RPEs (i.e., $\alpha_{IR+} = \alpha_{IR-} = \alpha_{SR+} = \alpha_{SR-} = 0.05$). As shown in Figure 3C, this agent also minimized selection of the "abnormal reaction". This may also be reasonable, as this agent combined rigorous normative model-free TD leaner and approximation of normative TD leaner. We then examined the behavior of agent having appetitive SR- and aversive IR-based systems by setting $\alpha_{SR+} = \alpha_{IR-} = 0.09$ and $\alpha_{SR-} = \alpha_{IR+} = 0.01$. Figure 3D show the results. As shown in Figure 3D-top, different from the previous cases, the $Q_{abnormal} - Q_{other@relief}$ difference did not smoothly decrease but remained to fluctuate and sometimes even became positive, indicating that this agent continued to take the "abnormal reaction" and transition to the obsession state rather frequently, as actually appeared in Figure 3D-middle,bottom. In other words, obsession-compulsion cycle was often developed and enhanced in this agent, as we expected. We further examined cases with different learning rates while $\alpha_{SR+} + \alpha_{IR+}$ and $\alpha_{SR-} + \alpha_{IR-}$ (i.e., total learning rates from positive and negative RPEs, respectively) were kept constant at 0.1, finding that agent with large α_{SR+} & small α_{IR+} and small α_{SR-} & large α_{IR-} (i.e., appetitive SR- and aversive IR-based systems) could develop enhanced obsession-compulsion cycle (Figure 3E).

Modifications and variations in the models

We conducted simulations for longer times, and found that the enhanced obsession-compulsion cycle developed in the agent with appetitive SR- and aversive IR-based systems ultimately terminated (Figure 4A). We looked at the time evolution of variables, and found that the IR-system-specific values, as well as the weights for the SR-system-specific values, grew to large magnitudes, while the magnitudes of the integrated action values and the SR matrix remained small (Figure 4B). Because the weights for the SR-system-specific values became so large, update of the SR matrix could

cause large changes in the SR-system-specific values and thereby changes in the integrated values, whose impact could be quite large given the small magnitudes of the integrated values. This presumably triggered the termination of enhanced obsession-compulsion cycle. Indeed, if the rate of the update of SR matrix, which was so far fixed at 0.01, decreased over time and converged to 0, i.e., SR became rigid (c.f., [30]), enhanced obsession-compulsion cycle appeared to persist, despite the growth of the system-specific weights/values (Figure 4C,D). Considering neural implementation, however, such an unbounded growth of the weights/values may be implausible. As an alternative modification to the model, we introduced a small decay (forgetting) (c.f., [31, 32]) to the original model with update of SR matrix at the fixed rate 0.01. Specifically, the IR-system-specific values and the weights for the SR-system-specific values were assumed to decay at a constant rate (0.001) per each time step. Then, the growth of these values and weights was bounded, and enhanced obsession-compulsion cycle persisted (Figure 4E-G).

The reason for the stable persistence of enhanced obsession-compulsion cycle in the agent with appetitive SR- and aversive IR-based systems can be understood by looking at the action values and the SR matrix during the enhanced cycle (Figure 4F). The "other" action at the relief state had a positive value, and the abnormal reaction had a lower but still positive value. These positive values are considered to be shaped through asymmetric SR-based updates by RPEs generated when the agent took an action at the obsession state. Specifically, positive RPE upon transition to the relief state had large effects since α_{SR+} was large whereas negative RPE upon stay at the obsession state had small effects since α_{SR-} was small. Now, assume that the agent, developing enhanced obsession-compulsion cycle, exists at the relief state and happens to take the "other" action repeatedly, without taking the abnormal reaction. It is in fact the optimal policy, and because no reward or punishment is given as long as the agent only takes the "other" action, the value of the "other" action should approach, through RPE-based update, to 0, which is equal to the optimal value. However, this value, 0, is lower than the positive value of the abnormal reaction (even though it slowly decays). Therefore, as the agent repeatedly takes the "other" action more and more, ironically the abnormal reaction becomes more and more likely to be chosen. This pulls the agent back to enhanced obsession-compulsion cycle, away from the optimal policy.

In the environmental model used so far (developed by [6]) (Figure 2), there was only a single "other" action at each state. It is conceivable to assume multiple (different) "other" actions (Figure 5A). We examined the behavior of the dual-system agent with decay in modified environments where there were two or eight "other" actions at each state. When there were two "other" actions at each state (Figure 5B,C), agent with appetitive SR- and aversive IR-based systems still exhibited enhanced obsession-compulsion cycle, although the proportion of the obsession state decreased from the original case with a single "other" action. The value of the abnormal reaction in such agent was around 0 (purple line in Figure 5B middle), and so the abovementioned mechanism for enhanced obsession-compulsion cycle would barely hold. However, when there were eight "other" actions at each state (Figure 5D,E),

the value of the abnormal reaction became negative (purple line in Figure 5D middle) and obsession-compulsion cycle was hardly enhanced even in the appetitive SR & aversive IR agent. These results suggest that the reduced representation of actions other than the abnormal reaction and the compulsion in the original environmental model is essential for enhancement of obsession-compulsion cycle.

Behavior of the dual-system agent in the two-stage decision task

We examined how the agent with appetitive SR- and aversive IR-based systems behaved in the two-stage decision task [7], in comparison to the agent with SR-based system only that would correspond to healthy controls who had long memory traces for both positive and negative RPEs in the previous work [6]. Specifically, we simulated choice sequences of both agents 100 times for each using different pseudorandom numbers, and fitted them by the RL model weighing model-based and model-free controls developed in the original study [7] to estimate the parameter w that represents the degree of model-based control. As shown in the left panels of Figure 6A,B, the distribution of the estimated w for the agent with appetitive SR- and aversive IR-based systems (Figure 6B) was smaller than that for the agent with SR-based system only (Figure 6A) (Wilcoxon rank sum test, $p = 1.04\times10^{-7}$). In contrast, fitting of choices generated by the original RL model with balanced eligibility trace (λ = 0.4 for both positive and negative RPEs) and those generated by a modified model with imbalance trace (λ = 0.4 and 0 for positive and negative RPEs, respectively), both of which had the same degree of model-based control (w = 0.5), did not result in smaller estimated w in the latter, as shown in the left panels of Figure 6C,D (Wilcoxon rank sum test, $p = 0.5134$). Therefore, our expectation was again verified.

We further analyzed the choice pattern of each type of agent. The agent with appetitive SR- and aversive IR-based systems made a model-based-type choice, taking into account whether the occurred state transition was the common type or rare type, after reward was obtained but much less so after reward was not obtained (Figure 6B, right panel). In contrast, the SR-only agent, as well as the agents with balanced or imbalanced eligibility trace, made a model-based-type choice regardless of whether reward was obtained at the previous trial (Figure 6A,C,D, right panels).

Discussion

We have verified our two expectations: i) the agent with appetitive SR- and aversive IR-based systems could develop enhanced obsession-compulsion cycle, similarly to the agent having long / short eligibility traces for positive / negative RPEs examined in [6], and ii) fitting of behavior of the agent with appetitive SR- and aversive IR-based systems could result in smaller weights of model-based control than the SR-only agent in the two-stage decision task whereas eligibility-trace imbalance *per se* would not bias the estimation of the degree of model-based control. These results reconcile the recent suggestion of memory trace imbalance in OCD [6] with the long-standing suggestion that OCD is associated with impairment of model-based (goal-directed) control [1, 3-5], raising a possibility that opponent learning in model-based (SR-based) and model-free (IR-based) controls underlies obsession-compulsion. Our results predict that OCD patients tend to show model-based-type choice after receiving reward but less so after receiving no reward in the two-stage decision task (Figure 6B, right panel). This pattern looks similar to the actually observed pattern based on 48 OCD subjects reported in a study [3] (their Supplementary Figure 1), although not similar to the pattern based on 32 OCD subjects reported in their preceding study [2] (their Supplementary Figure S1). Statistical verification of this specific hypothesis will be needed. Also, there is a limitation of our model regarding the results in a different version of the two-sage task as we discuss below.

Implications of our results, in relation to other studies

As described in the Introduction, the opponent combination of appetitive SR- and aversive IR-based systems has recently been shown to perform well in certain dynamic environments [28]. Specifically, in a virtual reward navigation task in which reward location dynamically changed, the agent with appetitive SR- and aversive IR-based systems outperformed agents with other combinations. Moreover, implementation of such an appetitive SR & aversive IR combination in the cortico-basal ganglia pathways appears consistent with various physiological and anatomical findings (c.f., Figure 11 of [28]), including activations indicative of SR in limbic or visual cortices [15, 16] and preferential connections from limbic and visual cortices to the direct pathway of basal ganglia [18, 19]. These previous suggestions, together with the results of the present study that the opponent SR+IR combination could develop enhanced obsession-compulsion cycle, potentially explain a mystery shown in the recent work [6]. Specifically, in that work, fitting of even healthy people tended to result in shorter memory trace for negative (than positive) PEs, and the authors suggested that it could indicate human's proneness to OCD, but why human may have such a bias in the first place remained unexplained. We propose that the opponent SR+IR combination has been evolutionarily selected because it is advantageous under certain dynamic environments, at the cost of proneness to OCD.

We have shown that when the number of possible actions other than the abnormal reaction or the compulsion was increased, development of enhanced obsession-compulsion cycle declined. This

result suggests that a factor contributing to enhanced obsession-compulsion cycle is that alternative actions are represented in a dimension-reduced manner. Previous work [30] suggested that dimension-reduced SR could relate to addiction if it is rigid, i.e., not updated according to changes in the policy. In the present work, rigidness of SR was needed for stable retention of enhanced obsession-compulsion cycle in the original model without decay, although not for the modified model with decay. Taken together, dimension-reduction and rigidness of state/action representation could generally relate to psychiatric disorders/symptoms.

Our model does not specifically describe how the SR- and IR-based systems are arbitrated and how they are modulated by medical treatments. Serotonin has been suggested to be related to arbitration of model-based and model-free controls [3, 33], and recent work demonstrated that silencing of dorsal raphe serotonin neurons disrupted model-based control in outcome devaluation tasks [34]. Meanwhile, selective serotonin reuptake inhibitors (SSRIs) have been used for treatment of OCD, and one of the suggested mechanisms of its effectiveness is that SSRIs re-engage the brain system for model-based control [4]. Our modeling results indicate a possibility that OCD is linked to impairment of learning of SR-based (model-based) system particularly from negative RPEs, which could be caused by serotonin depletion and recovered by SSRIs. This possibility is potentially consistent with a previous result shown in [33] that diminishing serotonin signaling by tryptophan depletion appeared to impair model-based choice after no-reward but not after reward in the two-stage decision task (their Figure 2a, the left two panels), similarly to the pattern predicted by our model (Figure 6B right panel).

Limitations and perspectives

The abovementioned studies examining the two-stage decision task in OCD subjects [3] or subjects with tryptophan depletion [33] also examined a different, "punishment version" of the two-stage task, in which reward or no-reward outcomes in the original task were replaced with no-punishment or punishment outcomes. Different from the results in the reward version of the task, in the punishment version, OCD subjects did not show impaired model-based choice [3] and tryptophan depletion rather promoted model-based choice [33]. The environmental model that we used (developed by [6]) only contained punishment and cost, and so it can be said to have a similarity to the punishment version, rather than the reward version, but then the abovementioned arguments that our model is potentially consistent with the experimental results for the reward version would not hold. Nonetheless, even if the environmental model was altered in a way that punishment (-1) for the stay at the obsession state was replaced with no reward for the stay at the obsession state and reward (1) for all the other cases, the behavior of the dual-system agent without decay was largely preserved provided that the IR-system-specific values and the weights for SR-system-specific values were initialized to $1+\gamma+\gamma^2+...=1/(1-\gamma)=2$ instead of 0. But still, the lack of outcome-valence dependence is an important limitation of our model. It was suggested [33] that serotonin's possible role in representation of the

average reward rate [35] may be related to such outcome valence-dependent differential effects of tryptophan depletion. Exploration of how our model can be integrated into the average reward RL framework (c.f., [35]) is a possible future direction.

Our modeling results also appear not consistent with the result of a study examining generalization in OCD patients [36]. Using sensory preconditioning paradigm with monetary rewards and losses, this study reported that OCD patients generalized less from rewards, but not losses, than heathy controls (HCs). Looking at their results, in fact the HCs did not on average show significant generalization from rewards but showed chance-level choices, and the OCD patients significantly avoided the stimulus associated with a second stimulus that was later associated with stochastic (risky) gain and preferred the alternative stimulus associated with a second stimulus later associated with neutral outcome (Figure 3a of [36]). In the second-stimulus-outcome (gain/loss/neutral) association phase of the task, participants were required to "bid" on the presented stimulus and received feedback regardless of their bidding decisions, whereas no feedback was given in the final choice phase of the task. Given these task properties and observed choice patterns, we speculate that the task worked as a test for generalization of aversiveness associated with riskiness and/or loss of opportunity that arose when participants did not "bid" on reward-associated stimulus, and the OCD patients showed such a generalization of aversiveness while the HCs did not. As SR-based learning is more generalizable than IR-based one, the appetitive SR & aversive IR combination of our model predicts lager generalization from positive than negative RPEs in OCD, apparently opposite to the abovementioned conjecture.

However, this contradiction could potentially be resolved by considering recent findings of dopamine neuronal subpopulation representing threat PEs rather than RPEs and striatal subpopulations engaged in threat (rather than reward) learning/management, including the tail of the striatum (TS) and substantia nigra pars lateralis (SNL) in mice [37-39], and also dopamine neuronal subpopulations potentially representing error signals for aversive outcome [40] or reward-omission [41]. Specifically, if greater learning of SR-based system from positive than negative dopamine signals in OCD suggested by our model occurs not only in the canonical cortico-basal ganglia-dopamine circuit for reward RL but also in the circuits for RL of threat or aversiveness, potentially through common mechanisms for corticostriatal projection preferences, the latter could cause (over)generalization of threat or aversiveness, potentially in line with the abovementioned conjecture. Given that opponent SR- and IR-based learning of reward is advantageous in certain dynamic reward environment [28], opponent SR- and IR-based learning of threat/aversiveness should similarly be advantageous in certain dynamic threat/aversiveness environments and could thus be evolutionarily maintained, at the cost of possible maladaptive overgeneralization of threat/aversiveness. The existence of parallel circuits for PEs/RL of appetitive and aversive outcomes could also relate to the observed valence-dependence of model-based/free choice behavior in OCD subjects and subjects with tryptophan (serotonin) depletion [3, 33]. Elucidating how these circuits cooperate or compete would be crucial for understainding the circuit mechanisms of OCD, as well as the circuit mechanisms of intact value-based behavior.

Materials and Methods

Environmental model that describes possible enhancement of obsession-compulsion cycle

We adopted the environmental model developed by the previous study [6] that describes possible enhancement of obsession-compulsion cycle (Figure 2). There are two states, i.e., the relief state and the obsession state, and two available actions at each state, i.e., the "abnormal reaction" and the "other" action at the relief state and the "compulsion" and the "other" action at the obsession state. State transitions are determined as follows: at the relief state, taking the abnormal reaction always causes transition to the obsession state whereas taking the other action always causes stay at the relief state, and at the obsession state, taking the compulsion causes transition to the relief state and stay at the obsession state with 50% probability each whereas taking the other action causes transition to the relief state with 10% probability and stay at the obsession state with 90% probability. Taking the compulsion at the obsession state requires cost (negative reward) −0.01, and every stay at the obsession state imposes punishment (negative reward) −1; no other reward is assumed. The parameter values regarding state transitions and rewards are the same as those used in the previous work [6]. We also examined modified versions of the environmental model, in which there were two or eight "other" actions at each state (Figure 5A). Probabilities of state transitions for these multiple "other" actions were set to the same values for the "other" actions in the original model.

Agent having coupled SR- and IR-based systems

We adopted the model agent developed by the recent work [28] that has coupled SR- and IR-based systems (Figure 1C), with a modification that SR of actions (c.f., [11]) rather than SR of states was used in the present study because there were only two states in the environmental model. Each system developed the system-specific value of each action, and their average, referred to as the (integrated) action value, was used for action selection and TD-RPE calculation.

Action selection was made in a soft-max manner. Specifically, when there were multiple available actions A_i (i = 1, ..., n), whose action values were $Q(A_i)$, A_i was selected with probability $\exp(\beta Q(A_i)) / \Sigma_i\{\exp(\beta Q(A_i))\}$, where β was the inverse temperature parameter representing the degree of choice exploitation over exploration and was set to 10.

SARSA-type TD-RPE was used for the results presented in the figures. Specifically, when agent took action A_{t-1}, paid cost c (0.01 for the compulsion and 0 for all the other actions), received reward r (−1 if staying at the obsession state and 0 otherwise), transitioned to the next state, and took the next action A_t, SARSA-type TD-RPE $\delta = -c + r + \gamma Q(A_t) - Q(A_{t-1})$, where γ was the time discount factor and was set to 0.5, was calculated. We also examined the cases with Q-learning-type TD-RPE for the original agent and environmental models, and the main properties of agent's behavior shown in

Figure 3 were not largely changed. Along with TD-RPE, TD errors for SR features were calculated: $\mathbf{\Delta} = \mathbf{e}_{t-1} + \gamma\mathbf{M}_t, - \mathbf{M}_{t-1}$, where $\mathbf{e}_{t-1}$ was the vector that had elements corresponding to all the actions and the element corresponding to A_{t-1} was 1 and all the other elements were 0, and $\mathbf{M}_i$ ($i = t-1$ or t) was the A_i-corresponding row of the SR matrix $\mathbf{M}$.

IR-based system-specific value of A_{t-1}, $Q_{\mathrm{IR}}(A_{t-1})$, was updated based on the TD-RPE: $Q_{\mathrm{IR}}(A_{t-1}) \leftarrow Q_{\mathrm{IR}}(A_{t-1}) + \alpha_{\mathrm{IR}+}\delta$ (when $\delta \geq 0$) or $Q_{\mathrm{IR}}(A_{t-1}) + \alpha_{\mathrm{IR}-}\delta$ (when $\delta < 0$), where $\alpha_{\mathrm{IR}+}$ and $\alpha_{\mathrm{IR}-}$ were the learning rates in the IR-based system for positive (non-negative) and negative TD-RPEs, respectively. SR-based system-specific value of A_{t-1}, $Q_{\mathrm{SR}}(A_{t-1})$, was given by the dot product of the SR feature vector for A_{t-1}, i.e., $\mathbf{M}_{t-1}$, and the weight vector $\mathbf{w}$, i.e., $\mathbf{w}\cdot\mathbf{M}_{t-1}$. The weight $\mathbf{w}$ was updated based on the TD-RPE: $\mathbf{w} \leftarrow \mathbf{w} + \alpha_{\mathrm{SR}+}\delta\mathbf{M}_{t-1}$ (when $\delta \geq 0$) or $\mathbf{w} + \alpha_{\mathrm{SR}-}\delta\mathbf{M}_{t-1}$ (when $\delta < 0$), where $\alpha_{\mathrm{SR}+}$ and $\alpha_{\mathrm{SR}-}$ were the learning rates in the SR-based system for positive (non-negative) and negative TD-RPEs, respectively. The SR feature vector for A_{t-1}, $\mathbf{M}_{t-1}$, was updated based on the TD errors for SR features: $\mathbf{M}_{t-1} \leftarrow \mathbf{M}_{t-1} + \alpha_{\mathrm{feature}}\mathbf{\Delta}$, where $\alpha_{\mathrm{feature}}$ was the learning rate for feature update and was set to 0.01 except for the simulations shown in Figure 4C,D, in which $\alpha_{\mathrm{feature}}$ decreased over time according to 0.01/(1 + time-step/1000). For the simulations shown in Figure 4E-G and Figure 5, the IR-system-specific values for all the actions and all the elements of the weight vector for the SR system-specific values ($\mathbf{w}$) decayed at a constant rate (0.001), i.e., were multiplied by 0.999 at each time step.

Agent was initially placed at the relief state. The IR-system-specific values for all the actions were initialized to 0, and the weight vector for the SR system-specific values ($\mathbf{w}$) was initialized to $\mathbf{0}$. The SR matrix $\mathbf{M}$ was initialized to the identity matrix, i.e., the features corresponding to the own actions were initialized to 1 and all the other features were initialized to 0. 100 simulations were conducted for each condition. The value of the time discount factor ($\gamma = 0.5$) was the same as the one used in the previous work [6], and the ranges of the learning rates $\alpha_{\mathrm{IR}+}$, $\alpha_{\mathrm{IR}-}$, $\alpha_{\mathrm{SR}+}$, and $\alpha_{\mathrm{SR}-}$ were also determined in reference to the value of the learning rate used in that study (0.1) although because the average (rather than the sum) of the SR- and IR-based system-specific values was used for action selection and TD-RPE calculation, there was effectively a difference of two times. The value of the inverse temperature used in the simulations shown in the main text and figures ($\beta = 10$) was larger than the value used in the previous work ($\beta = 1$) [6]. If β was set to 1 in our original model without decay, the proportion that the agent was at the obsession state was rather high (≥ around 0.5 on average) in any combinations examined in Figure 3A-D (($\alpha_{\mathrm{SR}+}$, $\alpha_{\mathrm{SR}-}$, $\alpha_{\mathrm{IR}+}$, $\alpha_{\mathrm{IR}-}$) = (0, 0, 0.1, 0.1), (0.1, 0.1, 0, 0), (0.05, 0.05, 0.05, 0.05), and (0.09, 0.01, 0.01, 0.09)).

Simulation and fitting of the two-stage decision task

We simulated the behavior of the agent having a coupled SR- and IR-based systems in the two-stage decision task consisting of 201 trials [7]. There were two choice options at the first stage, and selection of one of them led to either of two pairs of second-stage options with 70% or 30%

probabilities whereas selection of the other first-stage option led to either of the two pairs with the opposite 30% and 70% probabilities. Selection of one of the second-stage options led to reward (size 1) or no-reward. The probability of reward for each second-stage option was determined according to Gaussian random walk with reflecting boundaries at 0.25 and 0.75, and it was implemented in a way that pseudo normal random numbers (mean 0, SD 0.025) was added to the probability at every trial and the probability was reflected at 0.25 and 0.75.

At every trial, choice was made in the soft-max manner with the degree of exploitation over exploration (inverse temperature) (β) set to 5 at both stages. SARSA-type TD-RPE for the first stage was calculated after the second-stage choice was determined: $\delta_k(1) = 0 + \gamma V(O_k(2)) - V(O_k(1))$, where $O_k(1)$ and $O_k(2)$ were chosen options for the first and second stages at the k-th trial, respectively, and $V(O)$ was the value of option O (i.e., average of SR- and IR-system specific values). γ was the time discount factor, and it was set to 1 (i.e., no temporal discounting). Then, after reward (R = 1 or 0) was determined, TD-RPE for the second stage was calculated: $\delta_k(2) = R + 0 - V(O_k(2))$, where $V(O_k(2))$ reflected $\delta_k(1)$-based update of the weights of the SR system-specific values. The IR-based system-specific value of each first- and second-stage option was initialized to 0 and updated based on the TD-RPEs. The SR-based system had the SR of the first- and second-stage options, and the SR-based system-specific value was given by the dot product of the SR feature vector for the corresponding action and the weights, which were updated based on TD-RPEs. The SR matrix was initialized to the one that assumed the random policy on second-stage choice and incorporated the actual stage-transition probabilities. At every trial, after stage transition occurred and second-stage option was determined, SR features for the chosen first-stage option was updated based on the TD errors for SR features with the learning rate 0.05. We considered agent that had appetitive SR- and aversive IR-based systems and agent that effectively had SR-based system only, for which the learning rates in each system for positive and negative TD-RPEs were set to (α_{SR+}, α_{SR-}, α_{IR+}, α_{IR-}) = (0.27, 0.03, 0.03, 0.27) and (0.3, 0.3, 0, 0), respectively, common to both stages, and conducted 100 simulations for each agent.

Generated choice sequences were individually fitted by the RL model weighing model-based and model-free controls developed in the original study [7]. The RL model had seven free parameters: a_1 and a_2 (learning rates for the first and second stages), b_1 and b_2 (inverse temperatures for the first and second stages), λ (eligibility trace, representing the degree with which the model-free value of first-stage option was updated based on the TD-RPE at the second stage), ρ (perseveration or switching at first-stage choices), and w (degree (weight) of model-based control, with the degree (weight) of model-free control set to ($1-w$)). Since a_1, a_2, λ, and w should normally be between 0 and 1, these variables were transformed into atanh($2x-1$), where x represents a_1, a_2, λ, or w, in the fitting process so that the range of exploration was effectively bound to [0 1]. For each choice sequence, we explored a set of parameters that maximized the log likelihood [42] by using the "fminsearch" function of MATLAB, with the initial parameter values set as (a_1, a_2, b_1, b_2, λ, ρ) = (0.3, 0.3, 5, 5, 0.2, 0.2) and w = 0.2, 0.5, and 0.8 (i.e., these three cases were examined) and the 'MaxFunEvals' and 'MaxIter' options

of this function set to both 10000. Among the three cases with different initial values of w, we selected a case that gave the maximum log likelihood, and if the "fminsearch" function terminated with "exitflag" 1 (meaning normal termination) in that selected case, the corresponding data (value of w) was included in the following analysis. This was true for 97 out of 100 simulations for both types of agent. We compared the obtained distribution of w for each type of agent by using the Wilcoxon rank-sum test (Mann Whitney U test).

We also simulated the behavior of the original RL model [7], as well as the behavior of a modified model with imbalanced eligibility trace, in the two-stage decision task. As for the original model, the parameters were set to (a_1, a_2, b_1, b_2, λ, ρ, w) = (0.3, 0.3, 5, 5, 0.4, 0.2, 0.5). The modified model had two parameters, λ_1 and λ_2, representing the eligibility trace for positive (non-negative) and negative TD-RPEs, respectively, instead of the single parameter λ in the original model, and they were set to (λ_1, λ_2) = (0.4, 0) to represent imbalanced trace; the other parameters were set to the same values as those set for the original model. 100 simulations were conducted for each model, and generated choice sequences were individually fitted by the original model in the same manner as in the case of the agent with coupled SR- and IR-based systems described above. For each choice sequence, among the three cases of fitting with different initial values of w, we again selected a case that gave the maximum log likelihood, and this time the "fminsearch" function terminated with "exitflag" 1 in that selected case for all of the 100 simulations for both models. We again compared the obtained distribution of w for each model by using the Wilcoxon rank-sum test.

Precisely speaking, our implementation of the RL model developed in [7] and its variant, used for the fitting and simulations mentioned above, could be slightly different from the original one. Specifically, we could not find how the model-based system estimated the transition probabilities when the frequencies of past occurrence of both types of transitions exactly matched in the original study, and we assumed that the model-based system estimated them as 50% and 50% in such situations.

In addition to the analyses mentioned above, we separately conducted 1000 simulations for each of the four types of agent, and analyzed the choice pattern, i.e., calculated the proportion of stay choice (i.e., choosing the same option as the one chosen at the previous trial) at the first stage depending on whether reward was obtained or not and whether common or rare transition was occurred at the previous trial (we increased the number of simulations to 1000 in order to obtain the average pattern more accurately).

Software and statistics

Simulations were conducted by using MATLAB, and its functions "rand" and "randn" were used to implement probabilities and pseudorandom numbers. Standard deviation (SD) of simulation data was normalized by n, and standard error of the mean (SEM) was approximately calculated as

SD/$\sqrt{n}$. The Wilcoxon rank-sum test (Mann Whitney U test) was conducted by using R (function "wilcox.test").

Code availability

Codes to generate the data presented in the figures will be made available at: https://github.com/kenjimoritagithub/sr101

References

1. Gillan CM, Papmeyer M, Morein-Zamir S, Sahakian BJ, Fineberg NA, Robbins TW, et al. Disruption in the balance between goal-directed behavior and habit learning in obsessive-compulsive disorder. Am J Psychiatry. 2011;168(7):718-26. Epub 20110515. doi: 10.1176/appi.ajp.2011.10071062. PubMed PMID: 21572165; PubMed Central PMCID: PMCPMC3533260.
2. Voon V, Derbyshire K, Rück C, Irvine MA, Worbe Y, Enander J, et al. Disorders of compulsivity: a common bias towards learning habits. Mol Psychiatry. 2015;20(3):345-52. Epub 20140520. doi: 10.1038/mp.2014.44. PubMed PMID: 24840709; PubMed Central PMCID: PMCPMC4351889.
3. Voon V, Baek K, Enander J, Worbe Y, Morris LS, Harrison NA, et al. Motivation and value influences in the relative balance of goal-directed and habitual behaviours in obsessive-compulsive disorder. Transl Psychiatry. 2015;5:e670. Epub 20151103. doi: 10.1038/tp.2015.165. PubMed PMID: 26529423; PubMed Central PMCID: PMCPMC5068758.
4. Robbins TW, Vaghi MM, Banca P. Obsessive-Compulsive Disorder: Puzzles and Prospects. Neuron. 2019;102(1):27-47. doi: 10.1016/j.neuron.2019.01.046. PubMed PMID: 30946823.
5. Gillan CM, Kosinski M, Whelan R, Phelps EA, Daw ND. Characterizing a psychiatric symptom dimension related to deficits in goal-directed control. Elife. 2016;5:https://doi.org/10.7554/eLife.11305. Epub 2016/03/01. doi: 10.7554/eLife.11305. PubMed PMID: 26928075; PubMed Central PMCID: PMCPMC4786435.
6. Sakai Y, Sakai Y, Abe Y, Narumoto J, Tanaka SC. Memory trace imbalance in reinforcement and punishment systems can reinforce implicit choices leading to obsessive-compulsive behavior. Cell Rep. 2022;40(9):111275. doi: 10.1016/j.celrep.2022.111275. PubMed PMID: 36044850.
7. Daw ND, Gershman SJ, Seymour B, Dayan P, Dolan RJ. Model-based influences on humans' choices and striatal prediction errors. Neuron. 2011;69(6):1204-15. doi: S0896-6273(11)00125-5 [pii] 10.1016/j.neuron.2011.02.027. PubMed PMID: 21435563; PubMed Central PMCID: PMCPMC3077926.
8. Dolan RJ, Dayan P. Goals and habits in the brain. Neuron. 2013;80(2):312-25. doi: 10.1016/j.neuron.2013.09.007. PubMed PMID: 24139036; PubMed Central PMCID: PMCPMC3807793.
9. Montague PR, Dayan P, Sejnowski TJ. A framework for mesencephalic dopamine systems based on predictive Hebbian learning. J Neurosci. 1996;16(5):1936-47. PubMed PMID: 8774460.
10. Schultz W, Dayan P, Montague PR. A neural substrate of prediction and reward. Science. 1997;275(5306):1593-9. PubMed PMID: 9054347.
11. Russek EM, Momennejad I, Botvinick MM, Gershman SJ, Daw ND. Predictive representations can link model-based reinforcement learning to model-free mechanisms. PLoS Comput Biol. 2017;13(9):e1005768. Epub 2017/09/25. doi: 10.1371/journal.pcbi.1005768. PubMed PMID:

28945743; PubMed Central PMCID: PMCPMC5628940.

12. Dayan P. Improving Generalization for Temporal Difference Learning: The Successor Representation. Neural Computation. 1993;5(4):613-24.
13. Momennejad I, Russek EM, Cheong JH, Botvinick MM, Daw ND, Gershman SJ. The successor representation in human reinforcement learning. Nat Hum Behav. 2017;1(9):680-92. Epub 2017/08/28. doi: 10.1038/s41562-017-0180-8. PubMed PMID: 31024137; PubMed Central PMCID: PMCPMC6941356.
14. Stachenfeld KL, Botvinick MM, Gershman SJ. The hippocampus as a predictive map. Nat Neurosci. 2017;20(11):1643-53. Epub 2017/10/02. doi: 10.1038/nn.4650. PubMed PMID: 28967910.
15. Garvert MM, Dolan RJ, Behrens TE. A map of abstract relational knowledge in the human hippocampal-entorhinal cortex. Elife. 2017;6:e17086. Epub 2017/04/27. doi: 10.7554/eLife.17086. PubMed PMID: 28448253; PubMed Central PMCID: PMCPMC5407855.
16. Russek EM, Momennejad I, Botvinick MM, Gershman SJ, Daw ND. Neural evidence for the successor representation in choice evaluation. bioRxiv. 2021;https://doi.org/10.1101/2021.08.29.458114. doi: https://doi.org/10.1101/2021.08.29.458114.
17. Lei W, Jiao Y, Del Mar N, Reiner A. Evidence for differential cortical input to direct pathway versus indirect pathway striatal projection neurons in rats. J Neurosci. 2004;24(38):8289-99. doi: 24/38/8289 [pii] 10.1523/JNEUROSCI.1990-04.2004. PubMed PMID: 15385612.
18. Wall NR, De La Parra M, Callaway EM, Kreitzer AC. Differential innervation of direct- and indirect-pathway striatal projection neurons. Neuron. 2013;79(2):347-60. doi: 10.1016/j.neuron.2013.05.014. PubMed PMID: 23810541; PubMed Central PMCID: PMCPMC3729794.
19. Lu J, Cheng Y, Xie X, Woodson K, Bonifacio J, Disney E, et al. Whole-Brain Mapping of Direct Inputs to Dopamine D1 and D2 Receptor-Expressing Medium Spiny Neurons in the Posterior Dorsomedial Striatum. eNeuro. 2021;8(1):ENEURO.0348-20.2020. Epub 20210122. doi: 10.1523/ENEURO.0348-20.2020. PubMed PMID: 33380525; PubMed Central PMCID: PMCPMC7877463.
20. Frank MJ, Seeberger LC, O'reilly RC. By carrot or by stick: cognitive reinforcement learning in parkinsonism. Science. 2004;306(5703):1940-3. doi: 1102941 [pii] 10.1126/science.1102941. PubMed PMID: 15528409.
21. Hikida T, Kimura K, Wada N, Funabiki K, Nakanishi S. Distinct roles of synaptic transmission in direct and indirect striatal pathways to reward and aversive behavior. Neuron. 2010;66(6):896-907. doi: S0896-6273(10)00379-X [pii] 10.1016/j.neuron.2010.05.011. PubMed PMID: 20620875.
22. Kravitz AV, Tye LD, Kreitzer AC. Distinct roles for direct and indirect pathway striatal neurons in reinforcement. Nat Neurosci. 2012;15(6):816-8. doi: nn.3100 [pii] 10.1038/nn.3100. PubMed PMID: 22544310.

23. Tai LH, Lee AM, Benavidez N, Bonci A, Wilbrecht L. Transient stimulation of distinct subpopulations of striatal neurons mimics changes in action value. Nat Neurosci. 2012;15(9):1281-9. doi: 10.1038/nn.3188. PubMed PMID: 22902719; PubMed Central PMCID: PMCPMC3951287.
24. Iino Y, Sawada T, Yamaguchi K, Tajiri M, Ishii S, Kasai H, et al. Dopamine D2 receptors in discrimination learning and spine enlargement. Nature. 2020;579(7800):555-60. Epub 20200318. doi: 10.1038/s41586-020-2115-1. PubMed PMID: 32214250.
25. Lee SJ, Lodder B, Chen Y, Patriarchi T, Tian L, Sabatini BL. Cell-type-specific asynchronous modulation of PKA by dopamine in learning. Nature. 2021;590(7846):451-6. Epub 20201223. doi: 10.1038/s41586-020-03050-5. PubMed PMID: 33361810; PubMed Central PMCID: PMCPMC7889726.
26. Skvortsova V, Palminteri S, Pessiglione M. Learning to minimize efforts versus maximizing rewards: computational principles and neural correlates. J Neurosci. 2014;34(47):15621-30. doi: 10.1523/JNEUROSCI.1350-14.2014. PubMed PMID: 25411490.
27. Groman SM, Keistler C, Keip AJ, Hammarlund E, DiLeone RJ, Pittenger C, et al. Orbitofrontal Circuits Control Multiple Reinforcement-Learning Processes. Neuron. 2019;103(4):734-46.e3. Epub 20190625. doi: 10.1016/j.neuron.2019.05.042. PubMed PMID: 31253468; PubMed Central PMCID: PMCPMC6893860.
28. Morita K, Shimomura K, Kawaguchi Y. Opponent learning with different representations in the cortico-basal ganglia circuits. eNeuro (accepted). 2022;https://doi.org/10.1101/2021.10.29.466375 (bioRxiv).
29. Sutton RS, Barto AG. Reinforcement Learning: An Introduction (Second Edition). Cambridge, MA: MIT Press; 2018.
30. Shimomura K, Kato A, Morita K. Rigid reduced successor representation as a potential mechanism for addiction. Eur J Neurosci. 2021;53(11):3768-90. Epub 2021/05/10. doi: 10.1111/ejn.15227. PubMed PMID: 33840120.
31. Morita K, Kato A. Striatal dopamine ramping may indicate flexible reinforcement learning with forgetting in the cortico-basal ganglia circuits. Front Neural Circuits. 2014;8:36. doi: 10.3389/fncir.2014.00036.
32. Kato A, Morita K. Forgetting in Reinforcement Learning Links Sustained Dopamine Signals to Motivation. PLoS Comput Biol. 2016;12(10):e1005145. Epub 2016/10/13. doi: 10.1371/journal.pcbi.1005145. PubMed PMID: 27736881; PubMed Central PMCID: PMCPMC5063413.
33. Worbe Y, Palminteri S, Savulich G, Daw ND, Fernandez-Egea E, Robbins TW, et al. Valence-dependent influence of serotonin depletion on model-based choice strategy. Mol Psychiatry. 2016;21(5):624-9. Epub 20150414. doi: 10.1038/mp.2015.46. PubMed PMID: 25869808; PubMed Central PMCID: PMCPMC4519524.
34. Ohmura Y, Iwami K, Chowdhury S, Sasamori H, Sugiura C, Bouchekioua Y, et al. Disruption of

model-based decision making by silencing of serotonin neurons in the dorsal raphe nucleus. Curr Biol. 2021;31(11):2446-54.e5. Epub 20210409. doi: 10.1016/j.cub.2021.03.048. PubMed PMID: 33838101.

35. Daw ND, Kakade S, Dayan P. Opponent interactions between serotonin and dopamine. Neural Netw. 2002;15(4-6):603-16. doi: 10.1016/s0893-6080(02)00052-7. PubMed PMID: 12371515.
36. Rouhani N, Wimmer GE, Schneier FR, Fyer AJ, Shohamy D, Simpson HB. Impaired generalization of reward but not loss in obsessive-compulsive disorder. Depress Anxiety. 2019;36(2):121-9. Epub 20181128. doi: 10.1002/da.22857. PubMed PMID: 30484928; PubMed Central PMCID: PMCPMC6945299.
37. Menegas W, Akiti K, Amo R, Uchida N, Watabe-Uchida M. Dopamine neurons projecting to the posterior striatum reinforce avoidance of threatening stimuli. Nat Neurosci. 2018;21(10):1421-30. Epub 20180903. doi: 10.1038/s41593-018-0222-1. PubMed PMID: 30177795; PubMed Central PMCID: PMCPMC6160326.
38. Akiti K, Tsutsui-Kimura I, Xie Y, Mathis A, Markowitz JE, Anyoha R, et al. Striatal dopamine explains novelty-induced behavioral dynamics and individual variability in threat prediction. Neuron. 2022;110(22):3789-804.e9. Epub 20220920. doi: 10.1016/j.neuron.2022.08.022. PubMed PMID: 36130595; PubMed Central PMCID: PMCPMC9671833.
39. Tsutsui-Kimura I, Uchida N, Watabe-Uchida M. Dynamical management of potential threats regulated by dopamine and direct- and indirect-pathway neurons in the tail of the striatum. bioRxiv. 2022;https://doi.org/10.1101/2022.02.05.479267.
40. Matsumoto M, Hikosaka O. Two types of dopamine neuron distinctly convey positive and negative motivational signals. Nature. 2009;459(7248):837-41. doi: nature08028 [pii] 10.1038/nature08028. PubMed PMID: 19448610; PubMed Central PMCID: PMCPMC2739096.
41. Ishino S, Kamada T, Sarpong G, Kitano J, Tsukasa R, Mukohira H, et al. Dopamine error signal to actively cope with lack of expected reward. Research Square. 2022;https://doi.org/10.21203/rs.3.rs-1391246/v1.
42. Daw ND. Trial-by-trial data analysis using computational models. In: Delgado M, Phelps EA, Robbins TW, editors. Decision Making, Affect, and Learning, Attention and Performance XXIII: Oxford University Press; 2011.

Figure legends

Figure 1

Dual-system agent having a coupled successor-representation(SR)-based system and individual-representation(IR)-based system, adopted from the previous study [28]. **(A)** Schematic illustrations of SR (left) and IR (right). In SR, action A_1 is represented by a set of "discounted cumulative occupancies" of its successor actions (including A_1 itself), i.e., (temporally discounted) cumulative frequencies with which each successor action is taken, starting from A_1, under a given policy in the environment. The widths of the arrows indicate the probabilities of state transitions (to state S_1 or S_2) and action selections (A_2 or A_3 at S_1 and A_4 or A_5 at S_2), and the darkness of each circle indicates the occupancy of each action. By contrast, in IR, action A_1 is represented just by itself, separately from other actions. **(B)** Different cortical regions/populations having SR or IR may unevenly target/activate the direct and indirect pathways of basal ganglia (BG), which have been suggested to be crucial for learning from positive and negative feedbacks, respectively. The line widths of the arrows indicate the suggested preferences of projections/activations described in the Introduction and [28]. **(C)** Dual-system agent incorporating the potentially uneven projections/activations from the cortical regions/populations having SR or IR to the BG pathways. Each of the SR-based system and the IR-based system develops the system-specific value of each action, and the average of the two system-specific values, named the integrated action value, is used for soft-max action selection and calculation of SARSA-type TD-RPEs. The TD-RPEs are used for updating the system-specific values (or more specifically, the IR-based system-specific values and the weights for the SR-based system-specific values), with the learning rates for the SR- and IR-based systems in the cases of positive (non-negative) and negative TD-RPEs, denoted as α_{SR+}, α_{SR-}, α_{IR+}, and α_{IR-}, can take different values.

Figure 2

Environmental model describing possible development of obsession-compulsion cycle, adopted from the previous study [6]. There are two states: the relief state and the obsession state. At the relief state, agent can take the "abnormal reaction" (to an intrusive thought, i.e., spontaneously arising anxiety e.g., about door lock), which induces a transition to the obsession state, or the "other" action (e.g., just ignore or forget about the intrusive thought), with which the agent stays at the relief state. At the obsession state, agent can take the "compulsion" action (e.g., confirms door lock), which requires a small cost (0.01) but induces a transition back to the relief state with a high probability (50%), or the "other" action, which requires no cost but induces a transition back to the relief state only with a small probability (10%). Every stay at the obsession state imposes punishment (negative reward −1).

Figure 3

Behavior of different types of dual-system agent. **(A)** Behavior of agent that effectively had IR-based

system only ((α_{SR+}, α_{SR-}, α_{IR+}, α_{IR-}) = (0, 0, 0.1, 0.1)). *Top*: An example of the time evolution of the difference in the action values of the "abnormal reaction" and the "other" at the relief state ($Q_{abnormal} - Q_{other@relief}$). *Middle*: The moving average (over the past 100 time steps) of the proportion that the agent was at the obsession state in the same example simulation. *Bottom*: The average of the moving-average proportion of the obsession state across 100 simulations (black line), presented with ±SD (gray thin lines). **(B)** Behavior of agent that effectively had SR-based system only ((α_{SR+}, α_{SR-}, α_{IR+}, α_{IR-}) = (0.1, 0.1, 0, 0)). **(C)** Behavior of agent having IR- and SR-based systems, both of which learned equally from positive and negative RPEs ((α_{SR+}, α_{SR-}, α_{IR+}, α_{IR-}) = (0.05, 0.05, 0.05, 0.05)). **(D)** Behavior of agent having appetitive SR- and aversive IR-based systems ((α_{SR+}, α_{SR-}, α_{IR+}, α_{IR-}) = (0.09, 0.01, 0.01, 0.09)). **(E)** Proportion of the obsession state during time-steps 4901~5000, averaged across 100 simulations, in various cases with different learning rates. The horizontal and vertical axes indicate the learning rates of the SR-based system from positive and negative RPEs (i.e., α_{SR+} and α_{SR-}), respectively, while $\alpha_{SR+} + \alpha_{IR+}$ and $\alpha_{SR-} + \alpha_{IR-}$ (i.e., total learning rates from positive and negative RPEs, respectively) were kept constant at 0.1.

Figure 4

Behavior of the original and modified dual-system agents in the long run. **(A)** Behavior of the original agent with appetitive SR- and aversive IR-based systems for 50000 time steps. The learning rates were set as (α_{SR+}, α_{SR-}, α_{IR+}, α_{IR-}) = (0.09, 0.01, 0.01, 0.09) (same for (A-F)). Arrangements are the same as those in Figure 3A-D. **(B)** Integrated action values, system-specific values/weights, and SR matrix of the original appetitive SR & aversive IR agent. *Top*: Integrated value of each action averaged across 100 simulations (brown: "other" at the relief state, purple: "abnormal reaction", black: "other" at the obsession state, red: "compulsion"; same below). *Middle*: Weights for SR-based system-specific values (top four lines) and IR-based system-specific values (bottom four lines) averaged across 100 simulations. *Bottom*: SR matrix at time step 5000 (left) and 50000 (right) averaged across 100 simulations. Each row indicates the SR of each action shown in the left, with the darkness of the squares indicating the discounted cumulative occupancies of the actions shown in the bottom. **(C,D)** Results for appetitive SR & aversive IR agent with a modification, in which the rate of the update of SR matrix decreased over time according to 0.01/(1 + time-step/1000). **(E,F)** Results for appetitive SR & aversive IR agent with another modification, in which the IR-based system-specific values and the weights for the SR-based system-specific values decayed at a constant rate (0.001 at each time step) while the rate of the update of SR matrix was fixed at 0.01 as in the original agent. **(G)** Average proportion of the obsession state during time-steps 49901~50000 for the modified agent with decay of values/weights, in various cases with different learning rates. Notations are the same as those in Figure 3E.

Figure 5

Behavior of the modified agent with decay of values/weights in the modified environmental model, in

which there were multiple other actions at each state. **(A)** Modified environmental model assuming multiple "other" actions at each state. **(B)** Behavior of the appetitive SR & aversive IR agent ((α_{SR+}, α_{SR-}, α_{IR+}, α_{IR-}) = (0.09, 0.01, 0.01, 0.09)) with decay of values/weights in the environment with two "other" actions at each state. *Top*: The average of the moving-average proportion of the obsession state across 100 simulations (black line), presented with ±SD (gray thin lines). *Middle*: Integrated action value averaged across 100 simulations (brown: average of "other" actions at the relief state, purple: "abnormal reaction", black: average of "other" actions at the obsession state, red: "compulsion"). *Bottom*: SR matrices averaged across 100 simulations, in which each row indicates the SR of "abnormal reaction" and "compulsion" and the mean SR of "other" actions at each state shown in the left (i.e., averaged across "other" actions at the same states), with the darkness of the squares indicating the discounted cumulative occupancies of "abnormal reaction" and "compulsion" and the summed discounted cumulative occupancies of "other" actions at each state shown in the bottom (i.e., summed across "other" actions at the same states). **(C)** Average proportion of the obsession state during time-steps 49901~50000 for the agent with decay of values/weights, in various cases with different learning rates. The color bar is the same as the one in Figure 4G. **(D,E)** Results for the cases where there were eight "other" actions at each state in the environmental model.

Figure 6

Behavior of the dual-system agent in the two-stage decision task, as compared to the agent with balanced or imbalanced memory trace. **(A,B)** Comparison between the agent having SR-based system only ((α_{SR+}, α_{SR-}, α_{IR+}, α_{IR-}) = (0.1, 0.1, 0, 0)) (A) and the agent having appetitive SR- and aversive IR-based systems ((α_{SR+}, α_{SR-}, α_{IR+}, α_{IR-}) = (0.09, 0.01, 0.01, 0.09)) (B). *Left panels*: Distributions of the estimated parameter representing the degree of model-based control (w) across 97 simulations (out of 100 simulations: see the Materials and Methods for details). *Right panels*: Proportion of stay choice (i.e., choosing the same option as the one at the previous trial) at the first stage depending on whether reward was obtained or not and whether common or rare transition was occurred at the previous trial. The bars indicate the average across 1000 simulations, and the error-bars indicate ±SEM. **(C,D)** Comparison between the RL model developed in the original two-stage task study [7] with balanced eligibility trace (λ = 0.4) (C) and a modified model with imbalanced eligibility trace ((λ_1, λ_2) = (0.4, 0) for positive and negative TD-RPE, respectively) (D). The degree of model-based control (w) was set to 0.5 in the simulations of both models. *Left panels*: Distributions of the estimated w across 100 simulations. *Right panels*: Mean (±SEM) proportion of stay choice at the first stage across 1000 simulations.

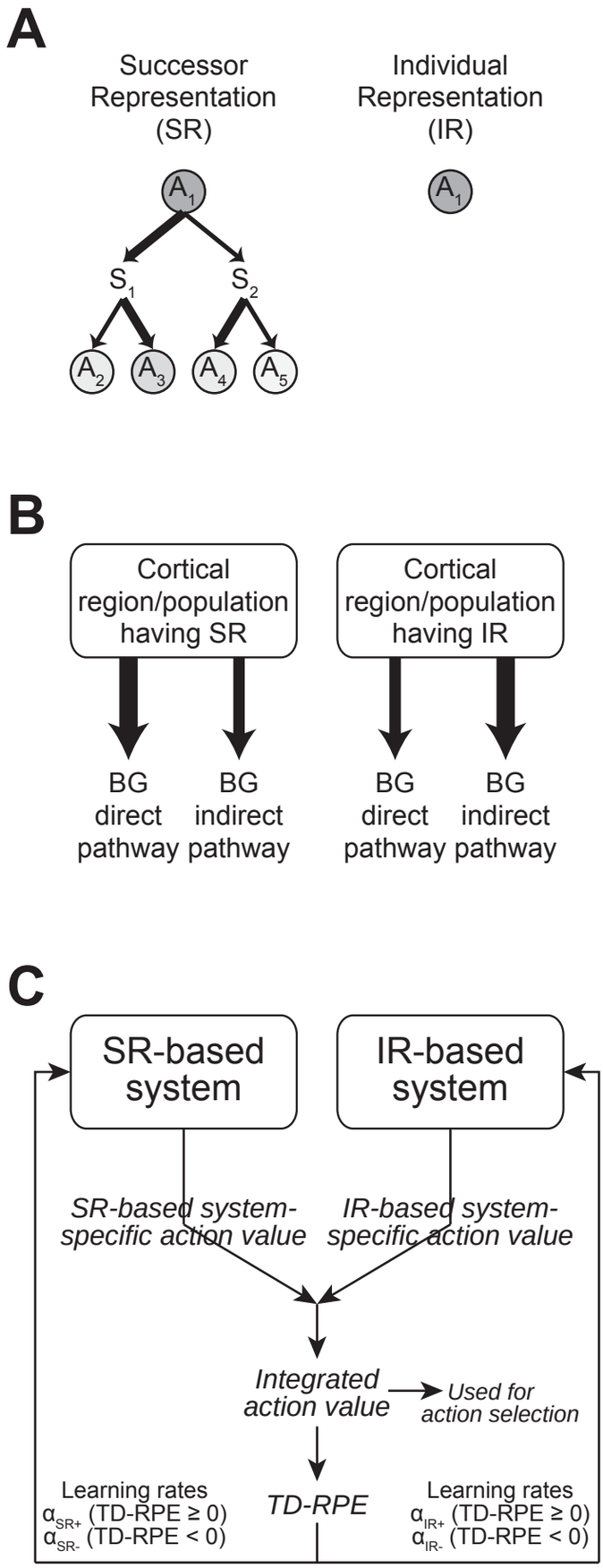
A
Successor Representation (SR)
Individual Representation (IR)
A1
S1
S2
A2
A3
A4
A5
A1
B
Cortical region/population having SR
Cortical region/population having IR
BG direct pathway
BG indirect pathway
BG direct pathway
BG indirect pathway
C
SR-based system
IR-based system
SR-based system-specific action value
IR-based system-specific action value
Integrated action value
Used for action selection
TD-RPE
Learning rates
αSR+ (TD-RPE ≥ 0)
αSR- (TD-RPE < 0)
Learning rates
αIR+ (TD-RPE ≥ 0)
αIR- (TD-RPE < 0)

Figure 1

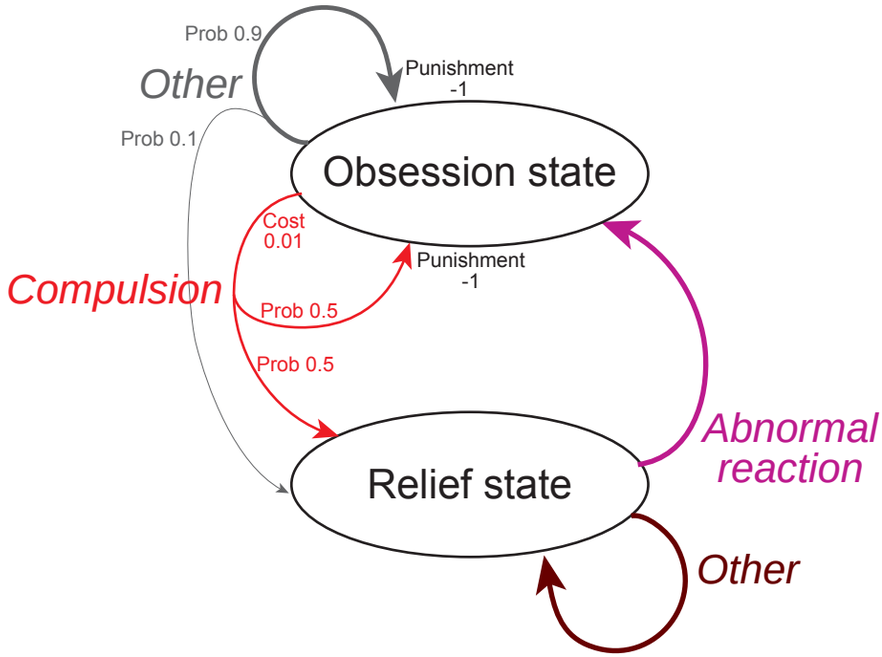
Prob 0.9
Other
Punishment
-1
Prob 0.1
Obsession state
Cost
0.01
Punishment
-1
Compulsion
Prob 0.5
Prob 0.5
Abnormal
reaction
Relief state
Other

Figure 2

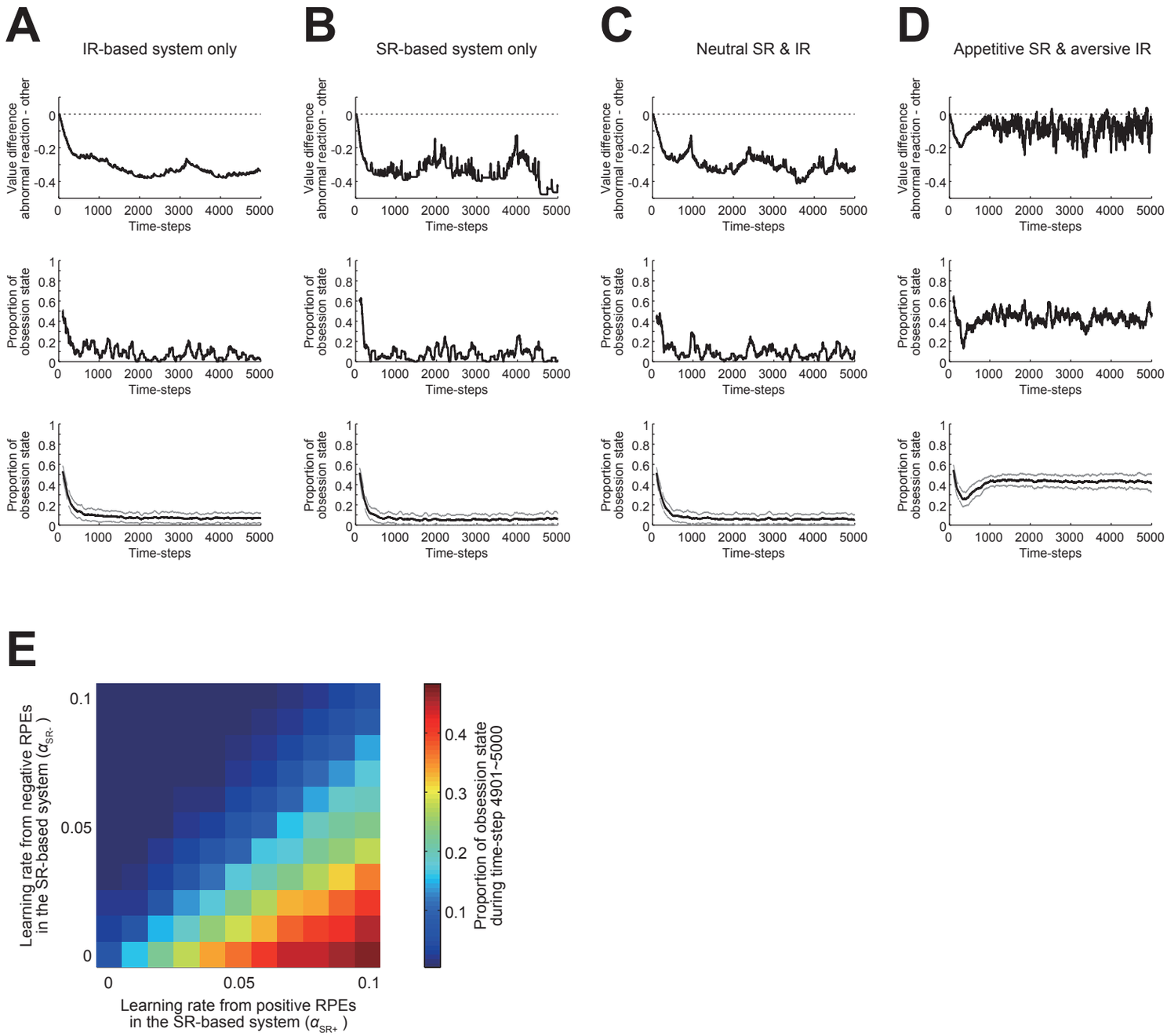
A
IR-based system only
B
SR-based system only
C
Neutral SR & IR
D
Appetitive SR & aversive IR
Value difference abnormal reaction - other
Proportion of obsession state
Time-steps
E
Learning rate from negative RPEs in the SR-based system (α_{SR-})
Learning rate from positive RPEs in the SR-based system (α_{SR+})
Proportion of obsession state during time-step 4901~5000

Figure 3

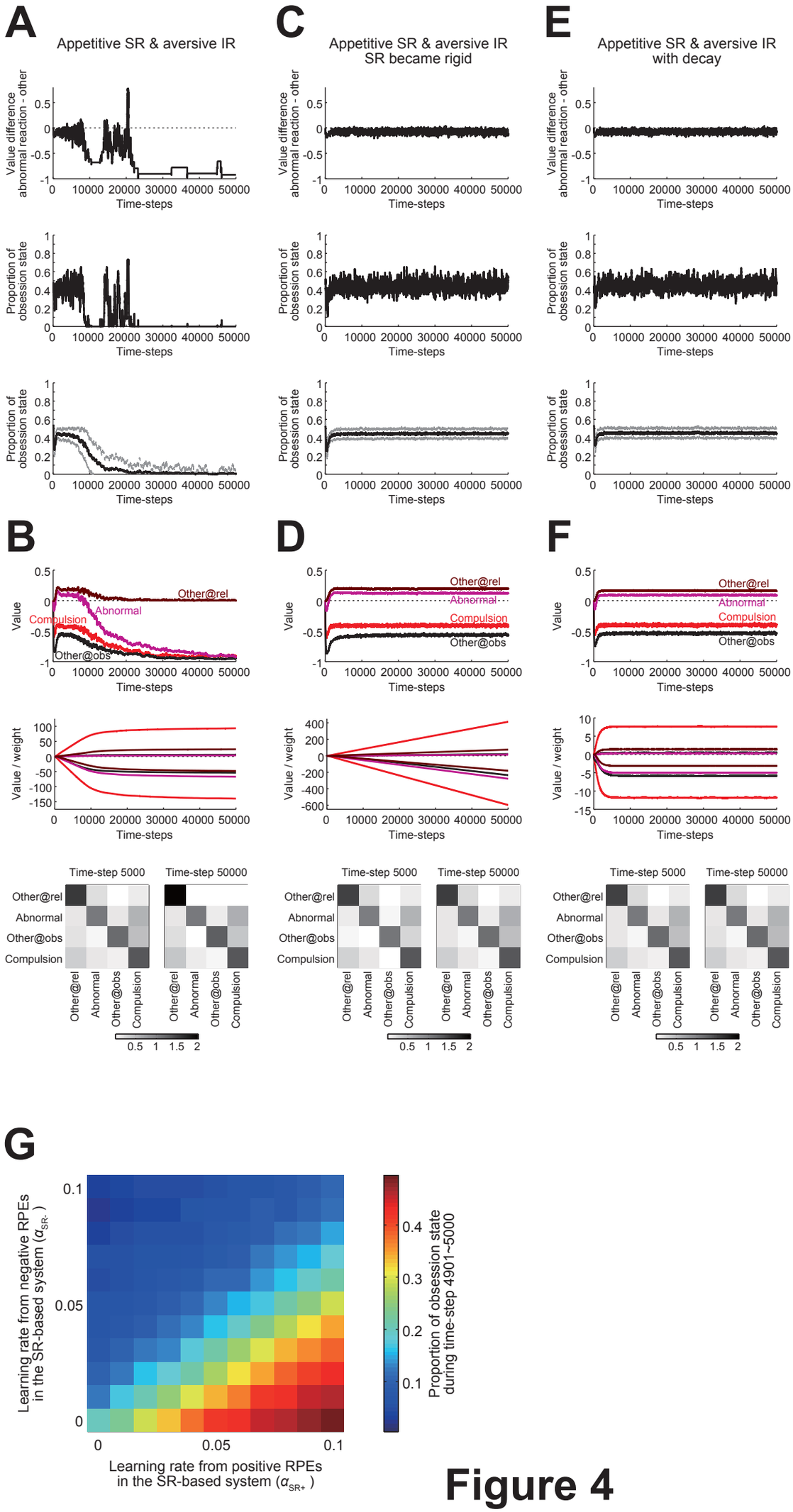
A
Appetitive SR & aversive IR
C
Appetitive SR & aversive IR
SR became rigid
E
Appetitive SR & aversive IR
with decay
Value difference
abnormal reaction - other
Proportion of
obsession state
Time-steps
B
D
F
Value
Value / weight
Other@rel
Abnormal
Compulsion
Other@obs
Time-step 5000
Time-step 50000
G
Learning rate from negative RPEs
in the SR-based system (α_{SR-})
Learning rate from positive RPEs
in the SR-based system (α_{SR+})
Proportion of obsession state
during time-step 4901~5000

Figure 4

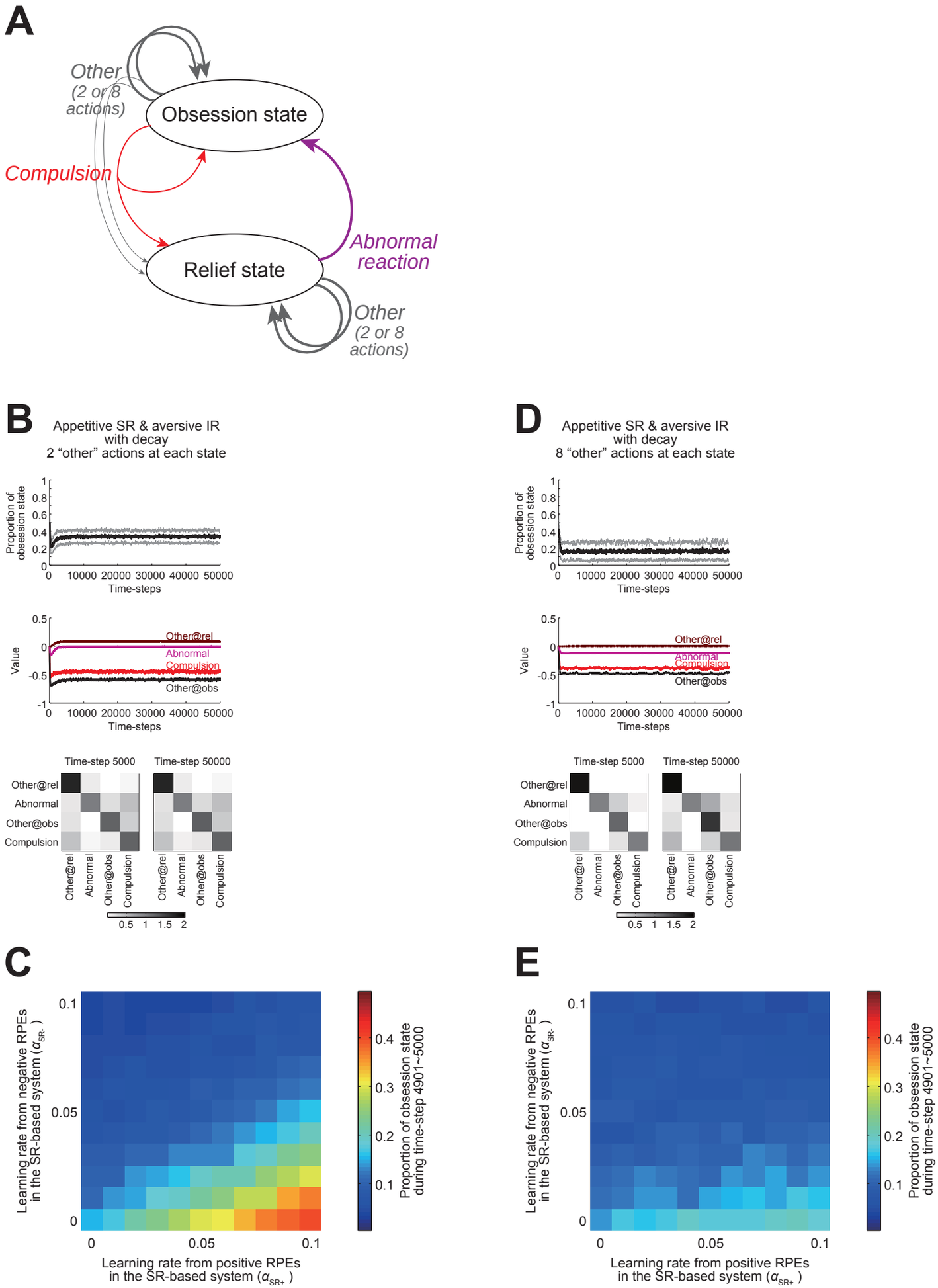
A
Other
(2 or 8
actions)
Obsession state
Compulsion
Abnormal
reaction
Relief state
Other
(2 or 8
actions)
B
Appetitive SR & aversive IR
with decay
2 "other" actions at each state
Proportion of
obsession state
Time-steps
Value
Other@rel
Abnormal
Compulsion
Other@obs
Time-step 5000
Time-step 50000
D
Appetitive SR & aversive IR
with decay
8 "other" actions at each state
C
E
Learning rate from negative RPEs
in the SR-based system (α_{SR-})
Learning rate from positive RPEs
in the SR-based system (α_{SR+})
Proportion of obsession state
during time-step 4901~5000

Figure 5

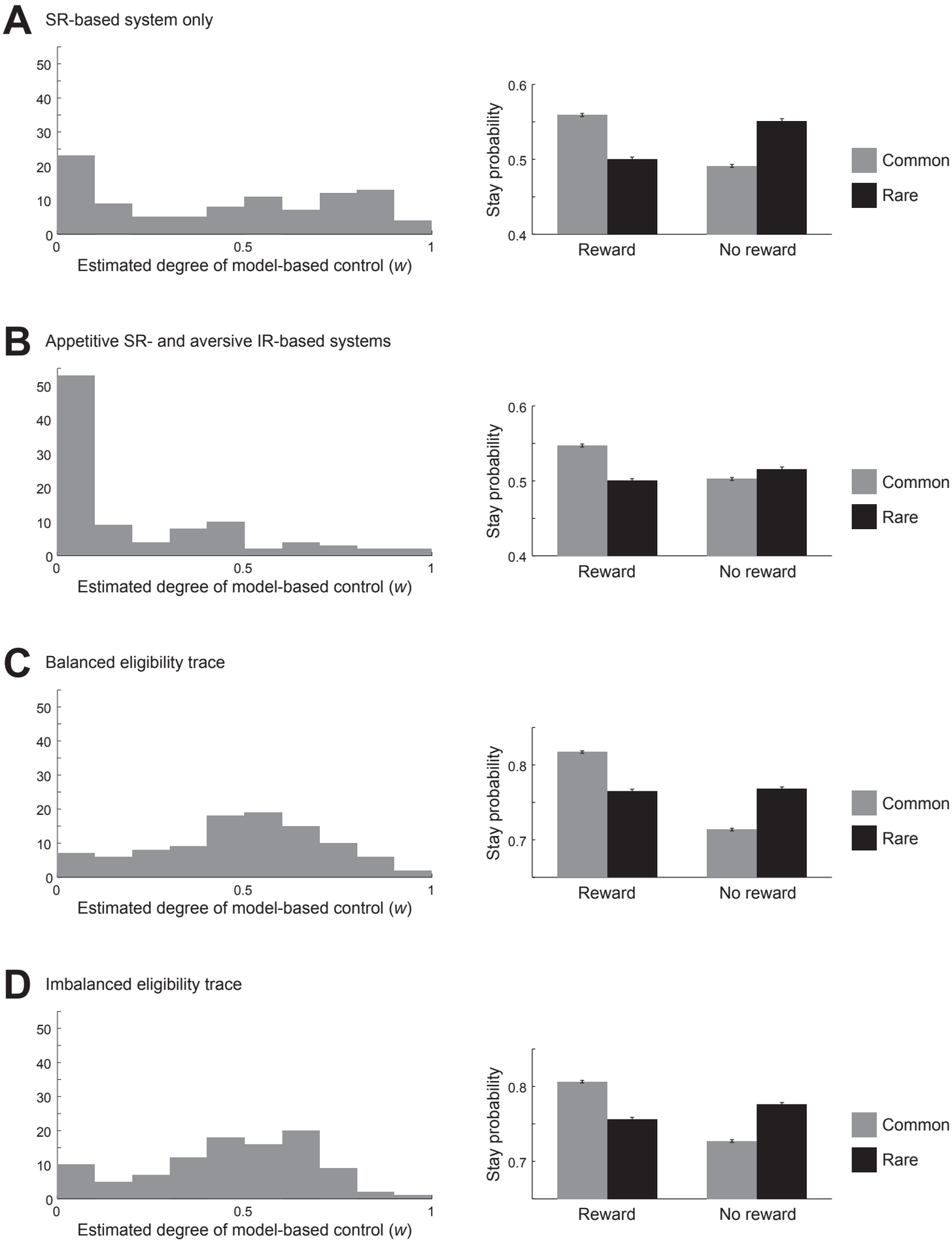
A
SR-based system only
Estimated degree of model-based control (w)
Stay probability
Reward
No reward
Common
Rare
B
Appetitive SR- and aversive IR-based systems
Estimated degree of model-based control (w)
Stay probability
Reward
No reward
Common
Rare
C
Balanced eligibility trace
Estimated degree of model-based control (w)
Stay probability
Reward
No reward
Common
Rare
D
Imbalanced eligibility trace
Estimated degree of model-based control (w)
Stay probability
Reward
No reward
Common
Rare

Figure 6